PNAS

Supporting Information for

The Rho guanine dissociation inhibitor α inhibits skeletal muscle Rac1 activity and insulin action

Lisbeth L. V. Møller, Mona S. Ali, Jonathan Davey, Steffen H. Raun, Nicoline R. Andersen, Jonathan Z. Long, Hongwei Qian, Jacob F. Jeppesen, Carlos Henriquez-Olguin, Emma Frank, Thomas E. Jensen, Kurt Højlund, Jørgen F.P. Wojtaszewski, Joachim Nielsen, Tim T. Chiu, Mark P. Jedrychowski, Paul Gregorevic, Amira Klip, Erik A. Richter, and Lykke Sylow

Corresponding author: Lykke Sylow
Email: Lykkesylow@sund.ku.dk

Co-corresponding author: Erik A. Richter
Email: Erichter@nexs.ku.dk

This PDF file includes:

Other supporting materials for this manuscript include the following:

Dataset S1

Supporting materials and methods

Cell cultures. Regular L6 myoblasts (RRID:CVCL_0385) and L6 muscle myoblasts stably overexpressing c-myc epitope-tagged Glucose Transporter Type 4 (GLUT4myc L6; RRID: CVCL_0P25) were grown in α-MEM medium (Gibco #22571-020) with 10% foetal bovine serum (Sigma-Aldrich #F0804), 100 units mL^{-1} penicillin, 100 µg mL^{-1}, and 0.25 µg mL^{-1} Gibco Amphotericin B (Gibco #15240-062) (5% CO_2, 37°C). Myoblasts were seeded and differentiated into multinucleated myotubes for the indicated time in α-MEM media with 2% foetal bovine serum, 100 units mL^{-1} penicillin, 100 µg mL^{-1}, and 0.25 µg mL^{-1} Gibco Amphotericin B.

Purification and characterization of the Flag-Rac1 interactome. C-terminal Flag-tagged (sequence DYKDDDDK (1)) Rac1 (Rac1-CTF, protein sequence: MQAIKCVVVGDGAVGKTCLLISYTTNAFPGEYIPTVFDNYSANVMVDGKPVNLGLWDTAGQEDY DRLRPLSYPQTDVFLICFSLVSPASFENVRAKWYPEVRHHCPNTPIILVGTKLDLRDDKDTIEKLK EKKLTPITYPQGLAMAKEIGAVKYLECSALTQRGLKTVFDEAIRAVLCPPPVKKRKRKCLLLDYKD DDDK) and N-terminal Flag-tagged Rac1 (Rac1-NTF, protein sequence: MDYKDDDDKMQAIKCVVVGDGAVGKTCLLISYTTNAFPGEYIPTVFDNYSANVMVDGKPVNLGL WDTAGQEDYDRLRPLSYPQTDVFLICFSLVSPASFENVRAKWYPEVRHHCPNTPIILVGTKLDLR DDKDTIEKLKEKKLTPITYPQGLAMAKEIGAVKYLECSALTQRGLKTVFDEAIRAVLCPPPVKKRK RKCLLL) were subcloned into a pMSCV-puro retroviral vector (Stratagene). Rac1 is a 192-amino acid protein (NCBI Reference Sequence: NP_033033.1 (2)) and with the Flag tag, the resulting proteins are with a predicted weight of ~22.5 kDa. For retrovirus production, Phoenix packaging cells were transfected with 10 µg of the retroviral vectors or GFP as a control. GFP-expressing cells were selected as the control to be able to visualize the efficiency of the infection and following puromycin-selection of the L6 myoblast when generating stable cell lines. After 48h, the viral supernatant was collected and filtered. Following infection of the regular L6 myoblasts with the retrovirus, cells expressing the ectopic virally encoded proteins were selected by incubation with 2 µg mL^{-1} puromycin. To verify that the Flag-tag did not affect Rac1 activity, Rac1-CTF, Rac1-NTF, GFP and regular L6 myoblasts were stimulated for 3 hours with 0.75 µg mL^{-1} Rac/Cdc42 Activator II (Cytoskeleton, Inc. #CN02). Rac1 activity was determined colorimetrically using a commercially available Rac1 G-LISA Activation Assay kit (Cytoskeleton, Inc. #BK126). For purification and characterization of the Flag-Rac1 interactome, Rac1-NTF and GFP L6 myoblasts were lysed in PBS with added protease inhibitor cocktail. After treatment with 1 mM GDP or 0.2 mM GTP-Y-S for 15 minutes at 30°C, the lysate was incubated with an anti-Flag antibody covalently attached to agarose (Anti-FLAG M2 Affinity gel; Sigma-Aldrich #A2220, RRID: AB_10063035), washed in a binding buffer, and eluted by incubating with 3x Flag peptide for 30 minutes (Sigma-Aldrich #F4799). The eluted proteins were digested by trypsin and subjected to reverse-phase liquid chromatography combined with tandem mass spectrometry (LC-MS/MS) using a high-resolution hybrid mass spectrometer (LTQ-Orbitrap, Thermo Scientific). The ratio of the amount of protein detected in the Rac1-GDP lysate (Rac1-GDP/GFP) or Rac1-GTP lysates (Rac1-GTP/GFP) compared to the control GFP lysate was determined. Proteins were excluded from the list of differentially bound proteins based on the inclusion criteria that the proteins had to be highly enriched in the Rac1-GDP Flag-immunopurified samples compared to a GFP control (>2-fold higher in Rac1-GDP lysate compared to control GFP) and that there was two or more peptide sequence similarity (single run, n=1). Fold changes of differentially bound proteins were calculated as Rac1-GTP/GFP compared to Rac1-GDP/GFP. Additionally, lysate containing Flag-Rac1 and the co-immunoprecipitated proteins was subjected to SDS-PAGE and the separated proteins were visualized by silver staining. Specific bands were excised and digested by trypsin and subjected to LC-MS/MS.

Generation of recombinant adeno-associated viral vectors. A cDNA construct encoding murine N-terminal Flag-tagged wildtype RhoGDIα or a RhoGDIα S101A mutant was synthesized and subcloned into a recombinant adeno-associated (AAV) expression plasmid consisting of a cytomegalovirus (CMV) promoter/enhancer and SV40 poly-A region flanked by AAV2 terminal

repeats (pAAV2) by Genscript (Piscataway, USA). Four shRNAs targeting RhoGDIα (5'-CCGGGAGTGGAATCTCACCATCAAACTCGAGTTTGATGGTGAGATTC-CACTCTTTTTG-3'; 5'-CCGGAGCTTCAAGAAACAGTCGTTTCTCGAGAAACGACTGTTTC-TTGAAGCTTTTTTG-3'; 5'-CCGGTCCGGCATGAAGTACATCCAACTCGAGTTGGATGTAC-TTCATGCCGGATTTTTG-3'; 5'-CCGGGCCTGGCCTGTCAGTATTTATCTCGAGATAAATA-CTGACAGGCCAGGCTTTTTG-3') were synthesized in a miR-155 backbone and subcloned into the pAAV2-CMV-MCS-SV40pA plasmid. Recombinant adeno-associated type-6 pseudotyped viral vectors (rAAV6) were generated as previously described (3, 4). In short, HEK293T cells were plated at a density of 8×10^6 cells onto a 15 cm culture dish and 8–16 h later co-transfected with 22.5 µg of a vector genome-containing plasmid and 45 µg of the packaging/helper plasmid pDGM6 using the calcium phosphate precipitate method. Seventy-two hours after transduction, cells and culture medium were collected and homogenized before 0.22 µm clarification (Millipore). The vector was purified from the clarified lysate by affinity chromatography using a HiTrap heparin column (GE Healthcare), ultracentrifuged overnight and resuspended in sterile Ringer's solution. The purified vector preparations were titred with a customized sequence-specific quantitative PCR-based reaction (Applied Biosystems) (Life Technologies).

siRNA transfection and rAAV6 transduction in GLUT4myc L6 cells. GLUT4myc L6 myoblasts were transfected with 70 nM siRNA targeting RhoGDIα (si-GDIα; Santa Cruz Biotechnology, Inc. #sc-36416) or control scramble siRNA (si-Ctrl; Santa Cruz Biotechnology, Inc. #sc-37007) for 7 hours using jetPRIME transfection reagent (Polyplus Transfection #114-15). After siRNA transfection, the cells were differentiated into multinucleated myotubes for 72 hours before measurement of Rac1 activity or GLUT4 translocation. Actin cytoskeleton remodelling was measured in day 7 myotubes, after siRNA double-transfection (100 nM) on day 0 and day 4. For rAAV6 transduction of GLUT4myc L6 cells, rAAV6-containing differentiation medium was added for 48 hours to day 2 myotubes and consisted of 5×10^{10} vector genomes (vg) mL^{-1} rAAV6:RhoGDIα WT, 2.5×10^{11} vg mL^{-1} rAAV6:RhoGDIα S101A or an empty vector (rAAV6:MCS) as a control. Rac1 activity or GLUT4 translocation was measured in day 7 myotubes. For rAAV studies with knockdown of endogenous RhoGDIα, siRNA double-transfection (100 nM) took place on day 0 and day 4 and rAAV6-containing differentiation medium was added for 48 hours to day 2 myotubes. Rac1 activity was measured in day 7 myotubes.

Rac1 activity assay, intracellular signaling and GLUT4 translocation in GLUT4myc L6 myotubes. GLUT4myc L6 myotubes were deprived of serum four hours prior to insulin stimulation. For measurement of Rac1 activity, myotubes were incubated ± insulin (10 nM or 100 nM) for 10 minutes. Rac1-GTP binding was determined colourimetrically using a commercially available Rac1 G-LISA Activation Assay kit (Cytoskeleton, Inc. #BK126) according to the manufacturer's instructions. In short, cells were lysed in lysis buffer with added protease inhibitor cocktail, supernatant collected by centrifugation (8792 x g) for 1 min at 4°C and the lysate was snap-frozen in liquid nitrogen. Protein concentration was determined in triplicate using bovine albumin standards, and 30 µg protein was loaded onto wells coated with the Rac1/Cdc42 binding domain (RBD) of PAK and incubated on a shaker for 30 minutes at 4°C. Bound Rac1 was determined colorimetrically using specific antibodies toward Rac1 and the optical absorbance was measured at 492 nm. Subsequently, total protein and intracellular signaling were determined by immunoblotting techniques. For immunoprecipitation of RhoGDIα, 4 µg of anti-RhoGDIα antibody (0.2 µg $µL^{-1}$; Table S1) was used on 100 µg protein lysate (lysis buffer containing 1% NP40, 10% glycerol) after being precleared with CL-6B for 30 minutes. For measurement of GLUT4 translocation, myotubes were incubated ± insulin (10 nM or 100 nM) for 15 minutes. For C2-ceramide treatment, cells were incubated with 25 µM C2-ceramide (Sigma-Aldrich #A7191) or as a control DMSO (0.125%) during the last 2 h of serum deprivation and the acute insulin challenge. Surface myc-tagged GLUT4 was measured as previously described with minor modifications (5). In short, cells were fixed in 3% paraformaldehyde, blocked in 5% goat serum, and surface myc-tagged GLUT4 was determined colourimetrically using an anti-c-Myc antibody (Table S1), horseradish peroxidase-conjugated secondary antibody and o-Phenylenediamine reagent. The

colorimetric reaction was stopped by adding 5N HCl and optical absorbance was measured at 492 nm.

Actin cytoskeleton remodeling in GLUT4myc L6 myotubes. For measurement of actin cytoskeleton remodeling, cells were seeded onto coverslips. GLUT4myc L6 myotubes were deprived of serum three hours prior to insulin stimulation. After incubation ± 100 nM insulin for 10 minutes, cells were fixed in 3% paraformaldehyde (in PBS supplemented with 0.68 mM $CaCl_2$, 0.49 mM $MgCl_2$) for 30 minutes on ice, quenched in 100 mM glycine (in PBS) for 20 minutes at room temperature, permeabilized with 0.1% TX-100 for 5 minutes at room temperature and blocked in 8% horse serum/2% BSA (in PBS) for 30 minutes at 37°C. Following incubation with a primary antibody targeting RhoGDIα (1:100 in 1:10 blocking solution; Table S1) for 2 hours at 37°C, the cells were stained with Alexa-488 goat anti-mouse IgG secondary antibody (1:1000 in 1:10 blocking solution; Thermo Fisher Scientific # A-11029, RRID: AB_2534088), DAPI (1:1000 in 1:10 blocking solution; Thermo Fisher Scientific # D1306), and rhodamine-phalloidin to visualize F-actin (1:500 in 1:10 blocking solution; Thermo Fisher Scientific # R415), for 45 minutes at 37°C. Coverslips were mounted in Agilent fluorescent mounting medium (Agilent #S302380-2). Images were captured with a Zeiss Axio Observer inverted microscope using a 100x 1.46 NA objective with an Andor iXon 885 EMCCD camera. Z-stacks were captured at 0. 2 µm intervals beyond the visible top and bottom of the rhodamine-phalloidin staining. For each condition, 20 images were captured. Cell surface ruffling was determined by nuclei midpoint offset determination (6), selecting the slice with the greatest area of nuclei as the midpoint. The cut-off point for the segmentation of dorsal ruffles was set at +5 slices above the midpoint of the nucleus. The bottom half of the Z-stacks was subjected to a maximum intensity projection, whereas the top, ruffle area of the Z-stacks was subjected to a sum intensity projection.

Ethical approval. All animal experiments complied with the European Convention for the protection of vertebrate animals used for experimental and other scientific purposes (No. 123, Strasbourg, France, 1985; EU Directive 2010/63/EU for animal experiments) and were approved by the Danish Animal Experimental Inspectorate.

Mouse Studies. All mice were maintained on a 12:12-h light–dark cycle and housed at 22 °C (with allowed fluctuation of ±2 °C) with nesting material. The mice were group-housed. The mice received a standard rodent chow diet (Altromin no. 1324; Brogaarden, Denmark) or a 60E% high-fat diet (HFD, no. D12492; Brogaarden, Denmark) as indicated and water ad libitum. Unless otherwise stated in the Materials and Methods or figure legends, female C57BL/6JBomTac mice (Taconic) were used for studies with rAAV6 administration.

Systemic and intramuscular administration of rAAV6 vectors. For systemic delivery studies, 1×10^{12} vg of rAAV6:RhoGDIα were administered in a volume of 100 µL Gelofusine (B. Braun, Germany) via the tail vein into C57BL/6JBomTac mice aged 4-7 weeks or C57BL/6NTac for the study Fig. 7D-H. The mice were fed a chow- or HFD for 8 weeks with the start of the diet intervention at rAAV6 administration. For intramuscular administration, C57BL/6JBomTac mice aged 8-12 weeks were placed under general anaesthesia (2% isofluorane in O_2). For overexpression studies, 1×10^{10} vg of rAAV6:RhoGDIα were administered in a volume of Gelofusine (TA/EDL: 30 µL; SOL/Gast: 50 µL; Tri: 30 µL) directly into the muscle compartments of one leg. Contralateral muscles were administered rAAV6:MCS. Insulin-stimulated glucose uptake was measured 4 weeks after rAAV6 administration as indicated. The mice were fed a chow- or HFD for 8 weeks before measurement of insulin-stimulated glucose uptake as indicated. For RhoGDIα knockdown studies, 1×10^{10} vg rAAV6:RhoGDIα shRNA were administered or as a control rAAV6:LacZ shRNA. Insulin-stimulated glucose uptake was measured 8 weeks after rAAV6 administration.

Morphological analyses. Body composition was analyzed using magnetic resonance imaging (EchoMRI-4in1TM, Echo Medical System LLC, Texas, USA). For systemic rAAV delivery studies, body composition was assessed at week 5 after rAAV6 administration.

Glucose tolerance test (GTT). For systemic rAAV delivery studies, blood glucose in the fed state was measured at 8 a.m. at week 0, 4 and 7 after rAAV6 administration. Glucose tolerance was measured in week 5. Prior to the test, the mice fasted for 6 hours from 7 a.m. D-mono-glucose (2 g kg^{-1} body weight) was administered intraperitoneal (i.p) and blood was collected from the tail vein and blood glucose concentration determined at time points 0, 30, 60, 90, and 120 minutes using a glucometer (Bayer Contour, Bayer, Switzerland). Incremental Area Under the Curve (AUC) from the basal blood glucose concentration was determined using the trapezoid rule for the first 60 minutes of the GTT. For measurement of plasma insulin, glucose was administered i.p. on a separate experimental day (4 days after the GTT) and blood was sampled at time points 0 and 20 minutes, centrifuged and plasma was quickly frozen in liquid nitrogen and stored at -20°C until processing. Plasma insulin was analyzed in duplicate (Mouse Ultrasensitive Insulin ELISA, #80-INSTRU-E10, ALPCO Diagnostics, USA).

Insulin tolerance test (ITT). For systemic rAAV delivery studies, insulin tolerance was assessed at week 7 after rAAV6 administration. Prior to the test, the mice fasted for 4 hours from 7 a.m. Insulin (0.5 U kg^{-1} body weight) was administered i.p. and blood was collected from the tail vein and blood glucose concentration determined at time points 0, 30, 60, 90, and 120 minutes using a glucometer (Bayer Contour, Bayer, Switzerland).

Indirect calorimetry. For systemic delivery studies, whole-body substrate utilization was assessed at weeks 6-7 after rAAV6 administration. Three days prior to the calorimetric measurements, mice were single-housed in specialized cages for indirect gas calorimetry but uncoupled from the PhenoMaster indirect calorimetry system (TSE PhenoMaster metabolic cage systems, TSE Systems, Germany). After a 2-day acclimation period coupled to the PhenoMaster indirect calorimetry system, oxygen consumption, CO2 production, habitual activity (beam breaks) and food intake were measured for 72 hours (TSE LabMaster V5.5.3, TSE Systems, Germany). On day 2, mice fasted followed by refeeding on day 3. The respiratory exchange ratio (RER) was calculated as the ratio between CO_2 production and oxygen consumption.

In vivo insulin-stimulated glucose uptake during retro-orbital insulin stimulation. To determine insulin-stimulated glucose uptake in the skeletal muscle of mice in intramuscular rAAV6 delivery studies, [^{3}H]-labelled 2-deoxyglucose ([^{3}H]-2DG; Perkin Elmer) was administered retro-orbitally (r.o.) in a bolus of saline containing 66.7 µCi mL^{-1} [^{3}H]-2DG (~32.4 Ci $mmol^{-1}$) corresponding to ~10 µCi/mouse (6 µL g^{-1} body weight), as described (7). The [^{3}H]-2DG saline bolus was with or without insulin (Actrapid, Novo Nordisk, Denmark). Decreased insulin clearance has been observed by us (7) and others in obese rodent (8, 9) and human (10) models. Therefore, to correct for changes in insulin clearance, 0.5 U kg^{-1} body weight of insulin was administered in chow-fed mice whereas only 0.4 U kg^{-1} body weight was administered to HFD-fed mice. Prior to stimulation, mice fasted for 4 hours from 7 a.m. Mice were anaesthetized 15 minutes before the r.o. injection (Chow/HFD: 7.5/9 mg pentobarbital sodium 100 g^{-1} body weight i.p.). Blood samples were collected from the tail vein immediately prior to and 5 and 10 minutes after r.o. injection. The blood was analyzed for glucose concentration using a glucometer (Bayer Contour, Bayer, Switzerland). At the 10 minutes time point, skeletal muscle (gastrocnemius, EDL, soleus, triceps brachii, and quadriceps) were excised, rinsed in saline, and quickly frozen in liquid nitrogen and stored at -80°C until processing. Blood was collected by punctuation of the heart, centrifuged and plasma was quickly frozen in liquid nitrogen and stored at -80°C until processing. Plasma samples were analyzed for insulin concentration and specific [^{3}H]-2DG activity. Plasma insulin was analyzed in duplicate (Mouse Ultrasensitive Insulin ELISA, #80-INSTRU-E10, ALPCO Diagnostics, USA). Tissue-specific 2DG-6-phosphate accumulation was measured as described (11, 12). To determine 2DG clearance from the plasma into the specific tissue, tissue-specific [^{3}H]-2DG-6-

phosphate was divided by AUC of the plasma-specific [^{3}H]-2DG activity at 0 and 10 minutes. To estimate tissue-specific glucose uptake (glucose uptake index), clearance was multiplied by the average blood glucose levels for the time points 0, 5, and 10 minutes. Tissue-specific glucose uptake was related to the weight of the analyzed muscle tissue and time.

Subcellular fractionation of rat skeletal muscle. Gastrocnemius and plantaris muscles were removed from the posterior hindlimb of fed male Wistar rats in the basal state and subjected to subcellular fractionation, as previously described and characterized in (13).

Human study. Muscle biopsies were from a euglycemic-hyperinsulinemic clamp in normal glucose-tolerant (NGT; BMI = 24 ± 1 kg m^{-2}), obese NGT (BMI = 33 ± 1 kg m^{-2}) and obese T2D (BMI = 33 ± 1 kg m^{-2}) subjects of mixed sex. The study from which the muscle biopsies were obtained has previously been published (14, 15). Due to unavailable muscle lysate for analysis, one subject from the NGT group was omitted compared to the original studies.

Histology. TA muscles from male mice were placed in cryomolds containing optimum cutting temperature cryoprotectant (Sakura #4583), frozen in liquid nitrogen-cooled isopentane and stored at -80°C. Cross-sections were cut at 10 µm thickness and fixed in methanol before hematoxylin and eosin staining to examine morphology as previously described with minor modifications (16). Stained sections were mounted using DePeX mounting medium (BDH). Images were captured with an Olympus BX53 microscope using a 40x 0.75 NA objective with an Olympus DP22 camera. For Flag-staining, muscles were cut at 8 µm thickness and mounted on positively charged glass slides (Thermo Fisher Scientific). Cryosections were fixed in ice-cooled 4% PFA diluted in phosphate-buffered saline (PBS) for 10 min and washed 3 x 5 min with an immunobuffer solution (IB = 0.25 % BSA, 50mM glycine, 0.033 % saponin, and 0.05 % sodium azide diluted in PBS). Sections were permeabilized with 0.05 % Triton-X100 for 10 min, followed by three washes of 5 minutes with IB. The sections were then blocked for one hour in blocking PBS buffer containing 2% BSA (Merck) and 10% goat serum (Gibco #16210-064) followed by overnight incubation at 4°C with anti-Flag antibody (1:200 dilution; Table S1) diluted in IB. The next day, sections were washed three times for 10 min in IB and incubated with a secondary antibody conjugated with Alexa 488 (1:300 dilution) for 2 hours. Sections were washed three times for 10 minutes and mounted in Vectashield antifade medium (Vector Laboratories #H-1000).

Transmission electron microscopy. A longitudinal specimen of the TA muscle was fixed with 2.5% glutaraldehyde in 0.1 M sodium cacodylate buffer (pH 7.3). The fixed specimen was rinsed four times in 0.1 M sodium cacodylate buffer before being post-fixed with 1% osmium tetroxide (OsO_4) in 0.1 M sodium cacodylate buffer for 90 min at 4°C. After post-fixation, the muscles were rinsed twice in 0.1 M sodium cacodylate buffer at 4°C, dehydrated through a graded series of alcohol at 4–20°C, infiltrated with graded mixtures of propylene oxide and Epon at 20°C, and embedded in 100% Epon at 30°C. Ultra-thin (60 nm) sections were cut (using an Ultracut UCT ultramicrotome; Leica Microsystems, Wetzlar, Germany) in two depths (separated by 150 µm) and contrasted with uranyl acetate and lead citrate. Sections were examined and photographed in a pre-calibrated transmission electron microscope (Philips CM100, Philips, Eindoven, The Netherlands) and an Olympus Veleta camera (Olympus Soft Imaging Solutions, Münster, Germany). From each specimen, six longitudinally oriented fibres were photographed at 13,500X magnification in a randomized systematic order, including 12 images from the subsarcolemmal region and 12 images from the myofibrillar region.
The volumetric content of intermyofibrillar and subsarcolemmal mitochondria was estimated by point counting (17) using a grid size of 460 nm generating 256 points per image and expressed per myofibrillar space and fibre surface area, respectively. The mitochondrial cristae surface area per mitochondrial volume was estimated by counting intersections on test lines (17) using a grid size of 90 nm. The images were analysed by a set-up blinded investigator.

RNA extraction and quantitative real-time reverse transcriptase PCR. Total RNA was extracted from ~15 mg TA muscle from male mice using TRIzol (Life Technologies). Using the High-Capacity cDNA Reverse Transcription Kit with RNase Inhibitor (Life Technologies), 1 µg of RNA was reverse transcribed as per the manufacturer's protocol. For measurement of mRNA transcripts, SYBR Green primers were used (Sigma-Aldrich). Rac1, forward: 5'-CCGTCTTTGACAACTATTCTG-3'; reverse: 5'-CTGTCATAATCTTCTTGTCCAG-3'. RhoA, forward: 5'-CACCTTTATAAGTGATGGCTG-3'; reverse: 5'-ATATCCGCCACATAGTTTTC-3'. The content of pan-actin (forward: 5'-CTGGCTCCTAGCACCATGAAGAT-3'; reverse: 5'-GGTGGACAGTGAGGCCAGGAT-3') was used to normalize samples for analysis by the ΔΔCt method.

Protein extraction. Unless otherwise indicated, cells were lysed in ice-cold RIPA buffer (Sigma-Aldrich #R0278) supplemented with 20 mM β-glycerophosphate, 10 mM NaF, 2 mM phenylmethylsulfonyl fluoride (PMSF), 2 mM Na_3VO_4, 10 µg mL^{-1} leupeptin, 10 µg mL^{-1} aprotinin, and 3 mM benzamidine. Supernatants were collected by centrifugation (8792 g) for 10 min at 4°C. Except for soleus and EDL, muscles and non-muscle tissues were crushed in liquid nitrogen prior to homogenization. All tissues were homogenized 2 x 30 sec at 30 Hz using a Tissuelyser II (Qiagen, USA) in ice-cold homogenization buffer (10% (v/v) Glycerol, 1% (v/v) NP-40, 20 mM Na-pyrophosphate, 150 mM NaCl, 50 mM HEPES (pH 7.5), 20 mM β-glycerophosphate, 10 mM NaF, 2 mM PMSF, 1 mM EDTA (pH 8.0), 1 mM EGTA (pH 8.0), 2 mM Na_3VO_4, 10 µg mL^{-1} Leupeptin, 10 µg mL^{-1} Aprotinin, 3 mM Benzamidine). After rotation end-over-end for 30 min at 4°C, lysate supernatants were collected by centrifugation (10,854 x g) for 15 min at 4°C.

Immunoblotting. Lysate protein concentration was determined using the bicinchoninic acid method using bovine serum albumin (BSA) standards and bicinchoninic acid assay reagents (Pierce). Immunoblotting samples were prepared in 6X sample buffer (340 mM Tris (pH 6.8), 225 mM DTT, 11% (w/v) SDS, 20% (v/v) Glycerol, 0.05% (w/v) Bromphenol blue). Protein phosphorylation (p) and total protein content were determined by standard immunoblotting technique loading equal amounts of protein. The polyvinylidene difluoride membrane (Immobilon Transfer Membrane; Millipore) was blocked in Tris-Buffered Saline with added Tween20 (TBST) and 2% (w/v) skim milk or 3-5% (w/v) BSA protein for 15 minutes at room temperature, followed by incubation overnight at 4°C with a primary antibody (Table S1). Next, the membrane was incubated with horseradish peroxidase-conjugated secondary antibody (Jackson Immuno Research) for 1 hour at room temperature. Bands were visualized using Bio-Rad ChemiDocTM MP Imaging System and enhanced chemiluminescence (ECL+; Amersham Biosciences). Densitometric analysis was performed using Image LabTM Software, version 4.0 (Bio-Rad, USA; RRID:SCR_014210). Coomassie brilliant blue staining (18), Ponceau S staining (19) or Memcode reversible protein stain (20) were used as loading controls.

Data analysis and visualization. Basal and insulin-stimulated samples were pooled when determining total protein content to increase the statistical power and accuracy of effect-size estimation. Tukey's post hoc test was used to evaluate significant one-way ANOVAs and interactions in two-way ANOVAs.
When applicable, cell culture experimental data were visualized using SuperPlots (21)**.** Each experimental round was symbol-coded with the small symbols representing wells and the large symbol the average of each experimental round.

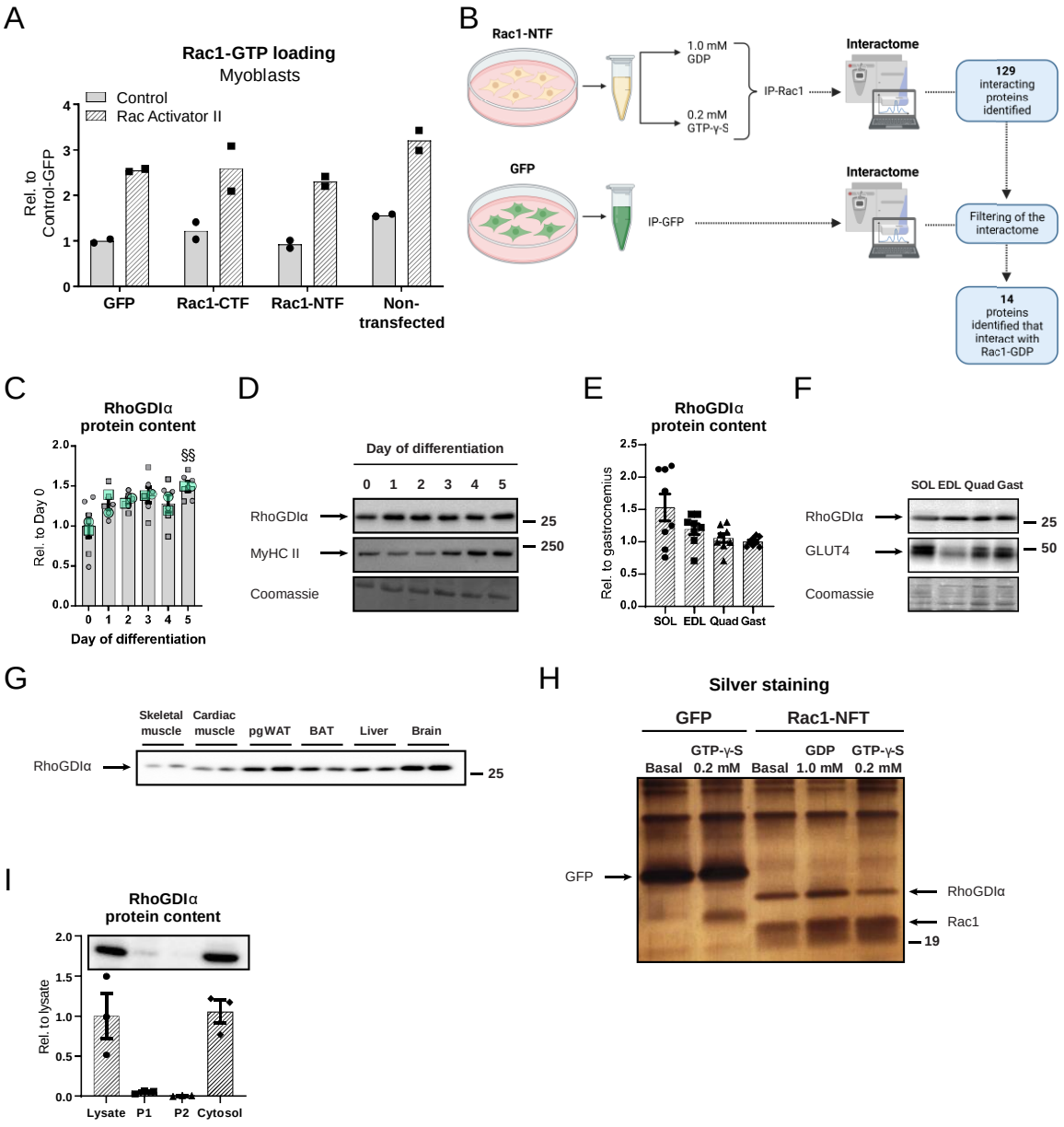

Figure S1. (A) Rac1 activity (Rac1-GTP loading) in non-transfected L6 myoblasts or L6 myoblasts expressing C-terminal (Rac1-CTF), N-terminal Flag-tagged Rac1 (Rac1-NTF), or GFP as a control ± 3 hours treatment with 0.75 µg/mL Rac Activator II. *n = 2*. Data are presented as mean with individual data points shown. (B) Schematic of the experimental workflow. Rat L6 myoblasts expressing Rac1-NTF (Rac1-NTF) or as a control GFP (GFP) were resuspended in PBS with added protease inhibitor cocktail and stimulated with GDP or GTP-γ-S for 15 minutes. Flag-tagged Rac1 was immunoprecipitated (IP) and the lysate with eluted co-immunoprecipitated proteins was subjected to proteomic analysis to determine the interactome. (C) RhoGDIα protein content in GLUT4myc L6 cells at day 0-5 of differentiation. As indicated by the SuperPlots (21), the experiment was assayed in triplicates and repeated twice. (D) Representative blots showing (C) and control coomassie staining. As a marker of differentiation, protein content of myosin heavy chain (MyHC) II increased over the five days of differentiation. (E) RhoGDIα protein content in

mouse (C57BL/6JBomTac) soleus (SOL), extensor digitorum longus (EDL), quadriceps (Quad), and gastrocnemius (Gast) muscles. The number of determinations in each group, *n = 8*. (F) Representative blots showing (E) with control coomassie staining. As a positive control (22–26), GLUT4 protein content was higher in the oxidative soleus muscle compared to the other investigated muscle. (G) RhoGDIα protein content in female and male mouse gastrocnemius muscle, cardiac muscle, perigonadal white adipose tissue (pgWAT), brown adipose tissue (BAT), liver, and brain. (H) Silver staining visualising the interaction between Rac1 and RhoGDIα. (I) Intracellular localization (lysate, pellet 1 [P1], P2 and cytosol) of RhoGDIα in rat posterior hindlimb (i.e., gastrocnemius and plantaris muscles). Markers of recycling endosomes, surface and intracellular membranes, t-tubule and mitochondria, enriched in P1 and P2 and sarcoplasmic reticulum marker enriched in P2 has been validated previously (13). *n = 3*.

Data were evaluated with a one-way ANOVA when applicable. Effect of time during differentiation §§ ($p<0.01$). Data are presented as mean ± S.E.M. with individual data points shown and for (C) the average from each experimental round.

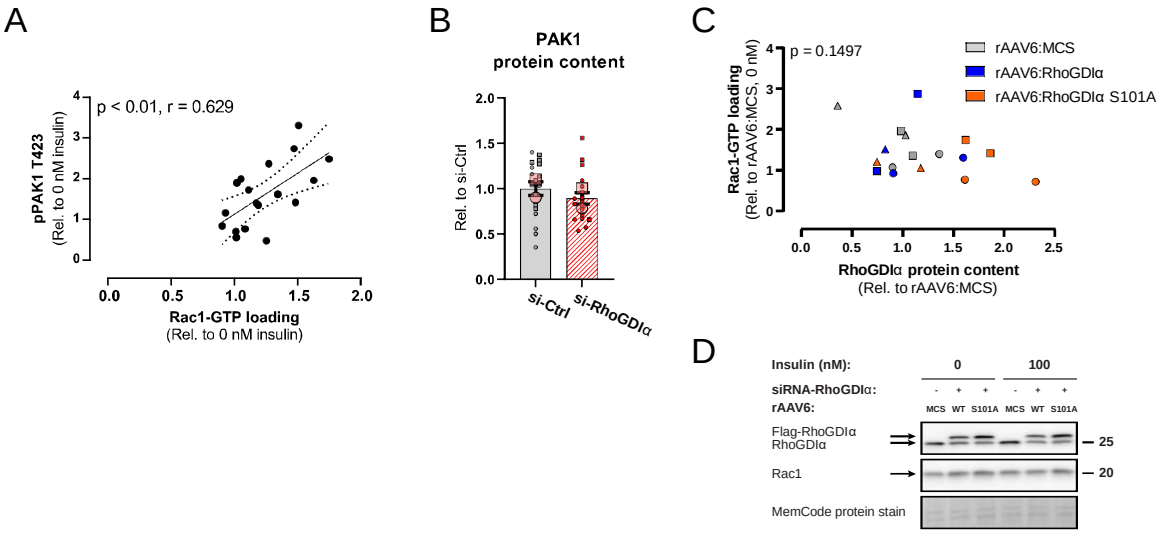

Figure S2. (A) Correlation between Rac1 activity (Rac1-GTP loading) and phosphorylated (p)PAK1 T423 in non-transfected GLUT4myc L6 myotubes. The cells were incubated ± 10 nM or 100 nM insulin for 10 minutes. The experiment was assayed in triplicates and repeated twice. Data were evaluated with Pearson's correlation. (B) PAK1 protein content in GLUT4myc L6 myotubes transfected with RhoGDIα siRNA (si-RhoGDIα) or control siRNA (si-Ctrl). As indicated by the SuperPlots (21), the experiment was assayed in triplicates and repeated twice. Data were evaluated with a Student's t-test. Data are presented as mean ± S.E.M. with individual data points shown and the average from each experimental round. (C) Correlation between Rac1 activity (Rac1-GTP loading) and RhoGDIα protein content in GLUT4myc L6 myotubes transfected with rAAV6:RhoGDIα or rAAV6:RhoGDIα S101A after siRNA-mediated knockdown of endogenous RhoGDIα. Control cells were transfected with rAAV6:MCS and control siRNA. The cells were incubated with 100 nM insulin for 10 minutes. The experiment was assayed in duplicates and repeated three times. Data were evaluated with Pearson's correlation. (D) Representative blots showing (Fig. 2G), (Fig. 2I), and control protein staining.

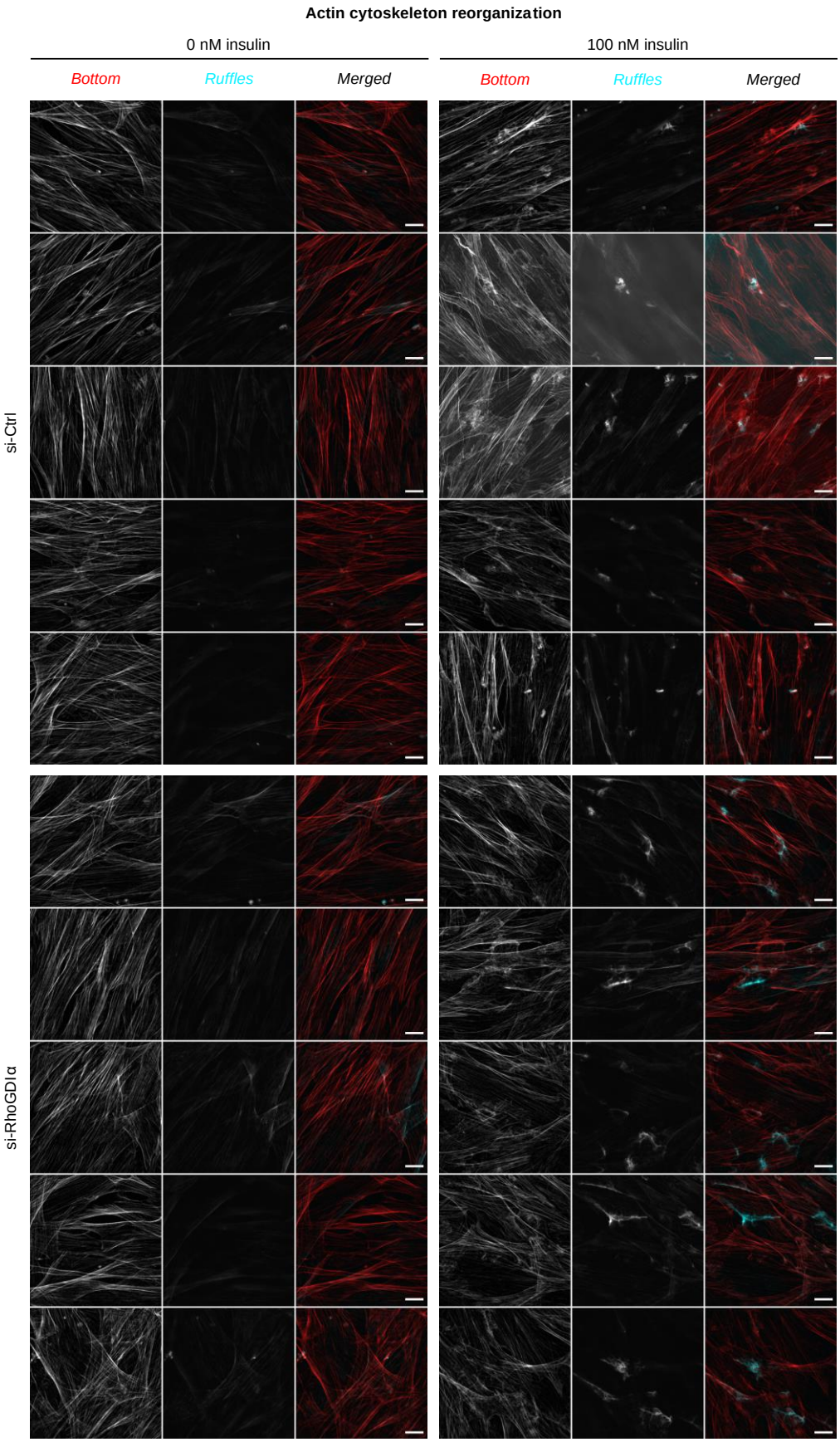
Actin cytoskeleton reorganization
0 nM insulin
100 nM insulin
Bottom
Ruffles
Merged
Bottom
Ruffles
Merged
si-Ctrl
si-RhoGDIα

Figure S3. Basal and insulin-stimulated actin cytoskeleton remodeling in GLUT4myc L6 myotubes transfected with RhoGDIα siRNA (si-RhoGDIα) or control siRNA (si-Ctrl) visualized using rhodamine-phalloidin. Bottom half of the Z-stacks (mainly stress fibres) subjected to a maximum intensity projection; Ruffles, top area of the Z-stacks subjected to a sum intensity projection. Five representative images shown of the 20 acquired images for each condition. Scale bar, 10 µm.

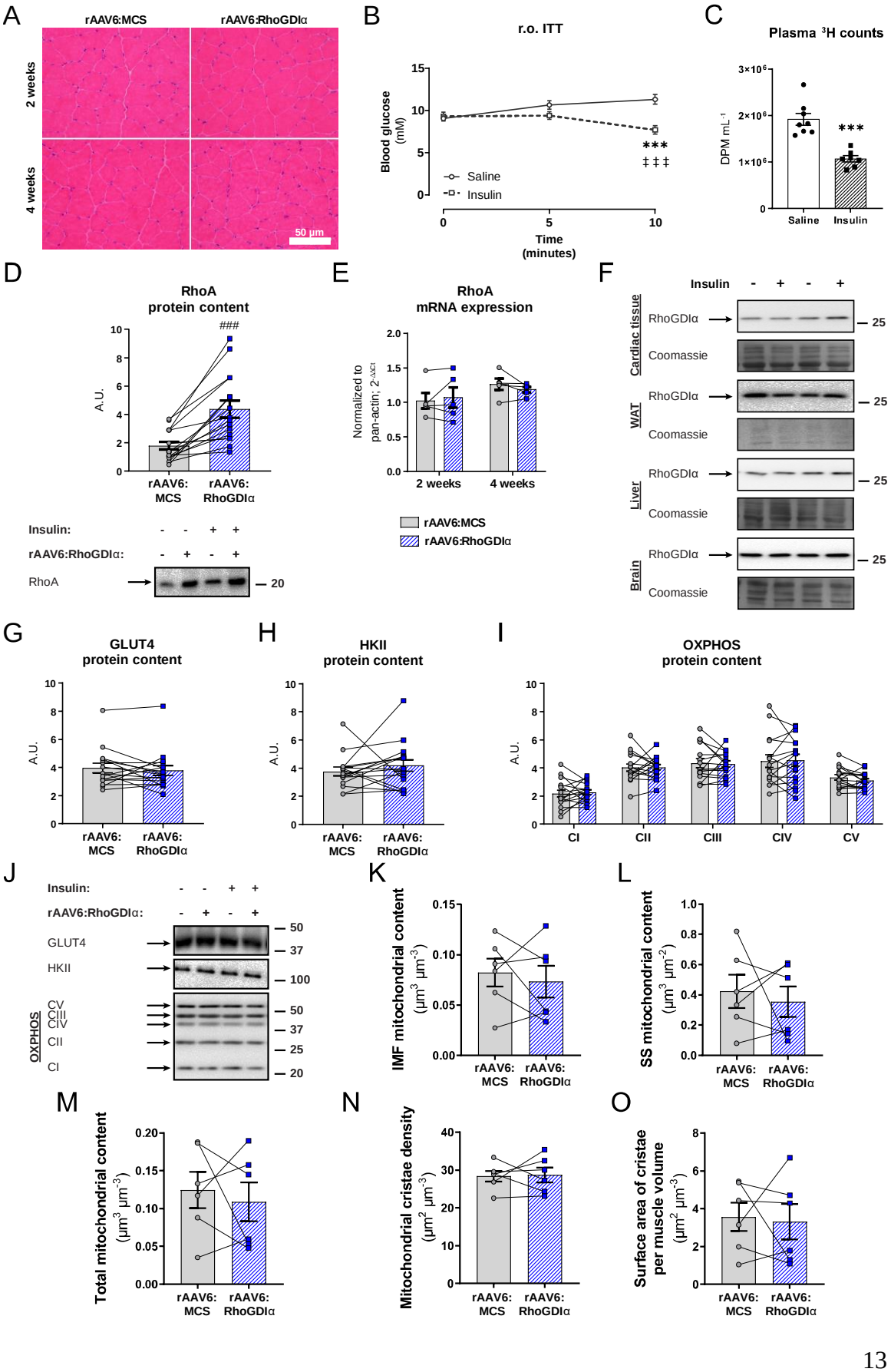
A
rAAV6:MCS
rAAV6:RhoGDIα
2 weeks
4 weeks
50 µm
B
r.o. ITT
Blood glucose (mM)
Saline
Insulin
***
‡‡‡
Time (minutes)
C
Plasma ³H counts
DPM mL⁻¹
***
Saline
Insulin
D
RhoA protein content
###
A.U.
rAAV6: MCS
rAAV6: RhoGDIα
Insulin:
rAAV6:RhoGDIα:
RhoA
E
RhoA mRNA expression
Normalized to pan-actin; 2^-ΔCt
2 weeks
4 weeks
rAAV6:MCS
rAAV6:RhoGDIα
F
Insulin
Cardiac tissue
WAT
Liver
Brain
RhoGDIα
Coomassie
G
GLUT4 protein content
H
HKII protein content
I
OXPHOS protein content
CI
CII
CIII
CIV
CV
J
GLUT4
HKII
OXPHOS
K
IMF mitochondrial content
L
SS mitochondrial content
M
Total mitochondrial content
N
Mitochondrial cristae density
O
Surface area of cristae per muscle volume

Figure S4. (A) Representative images of H&E-stained cross-sections in tibialis anterior (TA) muscles of male mice with recombinant adeno-associated viral vector encoding RhoGDIα (rAAV6:RhoGDIα) administered intramuscularly, while the contralateral muscle was injected with an empty viral vector (rAAV6:MCS), *n = 5*. Scale bar, 50 µm. (B) Blood glucose levels during a retro-orbital insulin tolerance test (r.o. ITT) in chow-fed mice (0.5 U kg^{-1} body weight). The number of mice in each group: Saline, *n = 8*; Insulin, *n = 7*. Data were evaluated with a two-way repeated measures (RM) ANOVA. (C) Plasma [^{3}H] counts at time point 10' during a r.o. ITT in chow-fed mice. Data were evaluated with a Student's t-test. (D) RhoA protein content in rAAV6:RhoGDIα- or rAAV6:MCS-treated gastrocnemius muscle. Data were evaluated with a paired t-test. (E) RhoA mRNA expression in rAAV6:RhoGDIα- or rAAV6:MCS-treated TA muscle 2 or 4 weeks after rAAV6-administration in chow-fed, male mice, *n = 4*. Data were evaluated with a paired t-test. (F) Representative blots showing RhoGDIα protein content and control coomassie staining in cardiac tissue, perigonadal white adipose tissue (WAT), liver, and brain. (G) GLUT4, (H) HKII, and (I) OXPHOS (subunits of mitochondrial oxidative phosphorylation complexes [CI: NDUFB8; CII: SDHB, CIII: UQCRC2; CIV: MTCO1, CV: ATP5A]) protein content in rAAV6:RhoGDIα- or rAAV6:MCS-treated gastrocnemius muscle. The number of mice in each group: Saline, *n = 8*; Insulin, *n = 7*. Total protein content was evaluated with a paired t-test. (J) Representative blots showing (G-I). (K-O) Mitochondrial content ((K) Intermyofibrillar [IMF]; (L) Subsarcolemmal [SS]; (M) Total), (N) mitochondrial cristae density and (O) mean surface area of cristae membrane per volume of fibre in rAAV6:RhoGDIα- or rAAV6:MCS-treated TA muscle. Data were evaluated with a paired t-test.

Significant interactions in two-way RM ANOVAs and significant t-tests: Effect of rAAV6:RhoGDIα vs. rAAV6:MCS ### ($p<0.001$); Effect of insulin *** ($p<0.001$); Insulin administration vs. time point 0' ‡‡‡ ($p<0.001$). Data are presented as mean ± S.E.M. or when applicable mean ± S.E.M. with individual data points shown. Paired data points are connected with a line. A.U., arbitrary units.

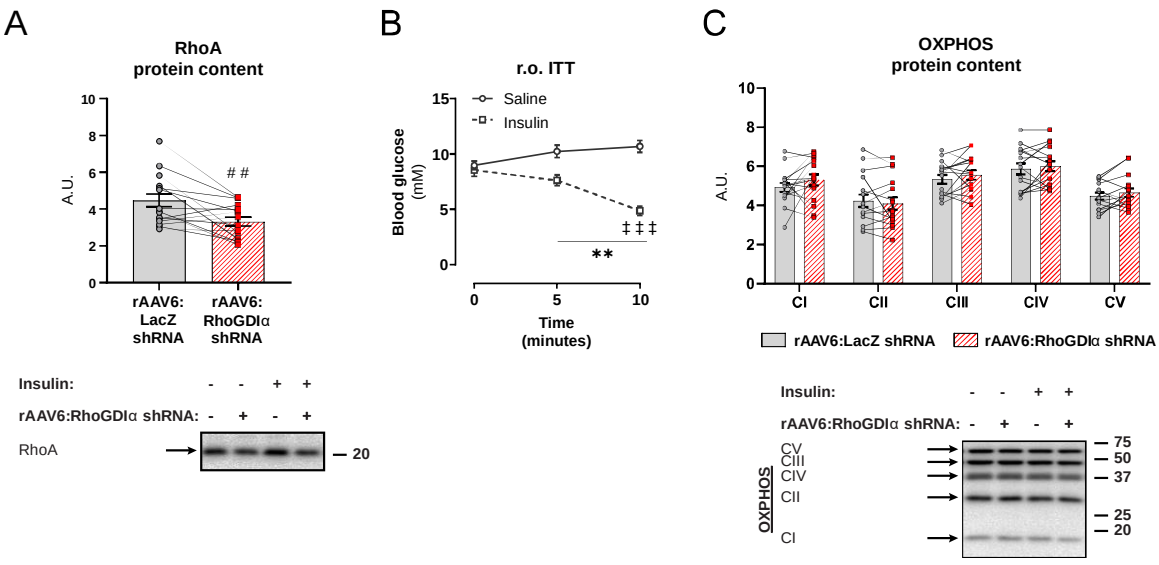

Figure S5. (A) RhoA protein content in gastrocnemius muscles with recombinant adeno-associated viral vector encoding RhoGDIα shRNA (rAAV6:RhoGDIα shRNA) administered intramuscularly, while the contralateral muscle was injected with a control vector (rAAV6:LacZ shRNA). The number of mice in each group: Saline, *n = 8*; Insulin, *n = 8*. (B) Blood glucose levels during a retro-orbital insulin tolerance test (r.o. ITT) in chow-fed mice (0.5 U kg^{-1} body weight). The number of mice in each group: Saline, *n = 8*; Insulin, *n = 8*. Data were evaluated with a two-way repeated measures (RM) ANOVA. (C) OXPHOS (subunits of mitochondrial oxidative phosphorylation complexes [CI: NDUFB8; CII: SDHB, CIII: UQCRC2; CIV: MTCO1, CV: ATP5A]) protein content and representative blots of gastrocnemius muscle injected with a recombinant adeno-associated viral vector encoding RhoGDIα shRNA (rAAV6:RhoGDIα shRNA) or a control vector (rAAV6:LacZ shRNA) for 8 weeks.

Total protein content was evaluated with a paired t-test. Significant interactions in two-way RM ANOVAs evaluated by Tukey's post hoc test and significant paired t-tests: Effect of rAAV6:RhoGDIα shRNA vs. rAAV6:LacZ shRNA ## ($p<0.01$); Effect of insulin ** ($p<0.01$); Insulin administration vs. time point 0' ‡‡‡ ($p<0.001$). Data are presented as mean ± S.E.M. or when applicable mean ± S.E.M. with individual data points shown. Paired data points are connected with a line. A.U., arbitrary units.

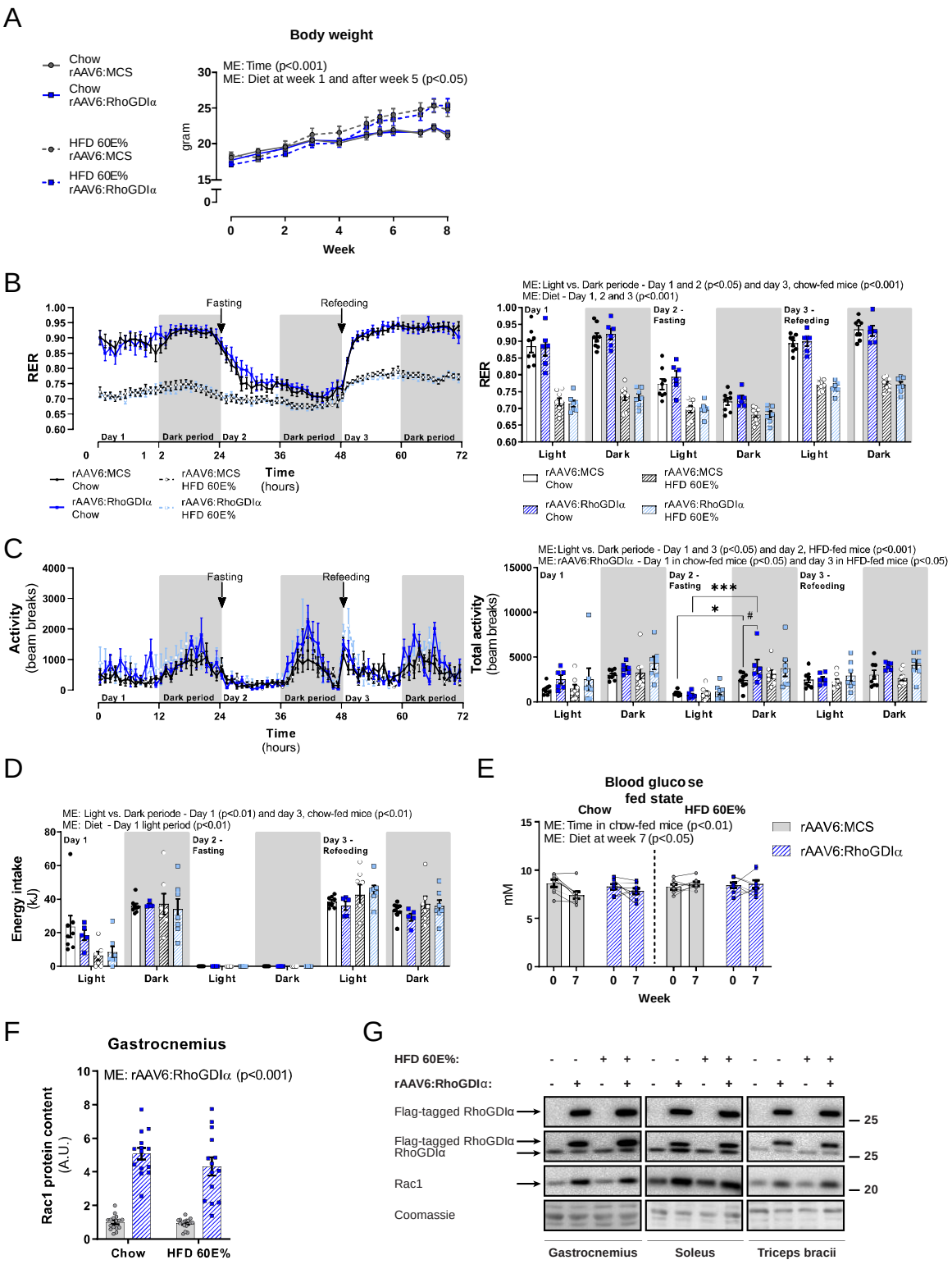

Figure S6. (A) Body weight of chow- or 60E% high-fat diet (HFD)-fed mice after recombinant adeno-associated viral vector-mediated overexpression of RhoGDIα (rAAV6:RhoGDIα) specifically in striated muscle after a single intravenous administration in young, adult mice. As a control, an empty vector was administered (rAAV6:MCS). The number of mice in each group: Chow, *n = 16/14* (rAAV6:MCS/rAAV6:RhoGDIα); HFD, *n = 16/14*. Start of diet intervention and rAAV6 administration

at week 0. Data were evaluated with two two-way repeated measures (RM) ANOVAs to test the factors 'rAAV6' (MCS vs. RhoGDIα) and 'time point' in chow- and HFD-fed mice, respectively. The effect of HFD was assessed with eight two-way ANOVAs to test the factors 'rAAV6' and 'diet' (Chow vs. HFD) at each time point, respectively. (B-D) Respiratory exchange ratio (RER; B), activity (beam breaks; C), and energy intake (D) during the light and dark period recorded over 72 hours in chow- or 60E% high-fat diet (HFD)-fed mice 6-7 weeks after rAAV6:RhoGDIα overexpression specifically in striated muscle after a single intravenous administration in mice. As a control, rAAV6:MCS was administered. The mice fasted on day 2 followed by refeeding on day 3. The number of mice in each group: Chow, *n = 8/6* (rAAV6:MCS/rAAV6:RhoGDIα); HFD, *n = 8/7*. Records of energy intake were missing for one rAAV6:RhoGDIα chow-fed mouse and rAAV6:MCS HFD-fed mouse. For day 1, data were evaluated with two two-way repeated measures (RM) ANOVAs to test the factors 'rAAV6' (MCS vs. RhoGDIα) and 'time of day' (Light vs. Dark) in chow- and HFD-fed mice, respectively. The effect of HFD was assessed with two two-way ANOVAs to test the factors 'rAAV6' and 'diet' (Chow vs. HFD) in the light and dark period, respectively. Day 2 and 3 were evaluated similarly. (E) Blood glucose concentration in the fed state (8 a.m.). The number of mice in each group: Chow, *n = 8/8* (rAAV6:MCS/rAAV6:RhoGDIα); HFD, *n = 7/8*. Data were evaluated with two two-way RM ANOVAs to test the factors 'rAAV6' (MCS vs. RhoGDIα) and 'time point' (week 0 vs. 7) in chow- and HFD-fed mice, respectively. The effect of HFD was assessed with three two-way ANOVAs to test the factors 'rAAV6' and 'diet' (Chow vs. HFD) at each time point, respectively. (F) Rac1 protein content in gastrocnemius muscle. The number of determinations in each group: Chow, *n = 16/14* (rAAV6:MCS/rAAV6:RhoGDIα); HFD, *n = 16/14*. Data were evaluated with a two-way ANOVA. (G) Representative blots showing RhoGDIα and Rac1 protein content with control coomassie staining in gastrocnemius, soleus, and triceps brachii muscle.

Main effects are indicated in the panels. Significant interactions in two-way (RM when applicable) ANOVA evaluated by Tukey's post hoc test: Light vs. dark period */*** ($p<0.05/0.001$); Effect of rAAV6:RhoGDIα # ($p<0.05$). Data are presented as mean ± S.E.M. or when applicable mean ± S.E.M. with individual data points shown. Paired data points are connected with a line. A.U., arbitrary units.

Table S1. Antibody Table.

Antibody name	Antibody ID (RRID)	Manufacturer; Catalog Number;	Species Raised in; Monoclonal or Polyclonal	Antibody dilution	Blocking buffer
Akt2	AB_2225186	Cell Signaling Technology; 3063	Rabbit, Monoclonal antibody	1:1000	2% milk
pAkt S474*	AB_329825	Cell Signaling Technology; 9271	Rabbit; Polyclonal antibody	1:1000	2% milk
pAkt T309*	AB_329828	Cell Signaling Technology; 9275	Rabbit; Polyclonal antibody	1:1000	2% milk
c-Myc#	AB_439680	Sigma-Aldrich; C3956	Rabbit; Polyclonal antibody	1:500	5% goat serum (in PBS+)
Flag	AB_262044	Sigma-Aldrich; F1804	Mouse; Monoclonal antibody	1:8000 (1:200ᵅ)	2% milk (IBᵅ)
GLUT4	AB_2191454	Thermo Fisher Scientific; PA1-1065	Rabbit; Polyclonal antibody	1:1000	2% milk
GSK-3β	AB_397601	BD Biosciences; 610202	Mouse; Monoclonal antibody	1:1000	2% milk
pGSK-3α/β S21/9	AB_329830	Cell Signaling Technology; 9331	Rabbit; Polyclonal antibody	1:2000	2% milk
HKII	AB_2295219	Santa Cruz Biotechnology; Sc-130358	Mouse; Monoclonal antibody	1:1000	2% milk
IRS1	AB_2127890	Millipore; 06-248	Rabbit; Polyclonal antibody	1 µg mL^{-1}	2% milk
MyHC II	AB_306073	Abcam; ab7784 ab7784	Mouse; Monoclonal antibody	1:80	2% milk
OXPHOS	AB_1622581	Abcam; MS604-300	Mouse; 5x Monoclonal antibodies	1:500	2% milk
PAK1	AB_330222	Cell Signaling Technology; 2602	Rabbit; Polyclonal antibody	1:500	2% milk
pPAK1/2 T423/402	AB_330220	Cell Signaling Technology; 2601	Rabbit; Polyclonal antibody	1:1000	3% BSA
Rac1	AB_397978	BD Biosciences; 610651	Mouse; Monoclonal antibody	1:1000	2% milk
RhoA	AB_10693922	Cell Signaling Technology; 2117	Rabbit; Monoclonal antibody	1:1000	2% milk

RhoGDIα	AB_2274313	Cell Signaling Technology; 2564	Rabbit; Polyclonal antibody	1:1000	2% milk
RhoGDIα	AB_2227516	Santa Cruz Biotechnology; sc-360	Rabbit; Polyclonal antibody	1:1000	5% BSA
RhoGDIα¤	AB_10917570	Santa Cruz Biotechnology sc-373724	Mouse; Monoclonal antibody	1:100	1:10 blocking solution
pRhoGDIα S101	AB_2059578	Santa Cruz Biotechnology; sc-33047	Rabbit; Polyclonal antibody	1:500	5% BSA
TBC1D4	AB_492639	Millipore; 07-741	Rabbit; Polyclonal antibody	1:1000	2% milk
pTBC1D4 T649**	AB_2651042	Cell Signaling Technology; 8881	Rabbit; Monoclonal antibody	1:1000	2% milk

* In mature skeletal muscle, the effects on insulin-stimulated glucose uptake seem mainly attributable to the Akt2 isoform (27–29), therefore nomenclature for Akt2 was used for pAkt S474 and T309 (equivalent to pAkt1 S473 and T308). ** Mouse nomenclature was used for pTBC1D4 T649 (equivalent to human T642). # Used for GLUT4 translocation assay. ¤ Used for immunofluorescence staining.

Dataset S1 (separate file). The list of total proteins identified in the Flag-Rac1 interactome in L6 myoblasts.

SI References

1. T. P. Hopp, *et al.*, A Short Polypeptide Marker Sequence Useful for Recombinant Protein Identification and Purification. *Bio/Technology 1988 610* **6**, 1204–1210 (1988).
2. N. A. O'Leary, *et al.*, Reference sequence (RefSeq) database at NCBI: current status, taxonomic expansion, and functional annotation. *Nucleic Acids Res.* **44**, D733–D745 (2016).
3. M. J. Blankinship, *et al.*, Efficient transduction of skeletal muscle using vectors based on adeno-associated virus serotype 6. *Mol. Ther.* **10**, 671–678 (2004).
4. C. E. Winbanks, *et al.*, Follistatin-mediated skeletal muscle hypertrophy is regulated by Smad3 and mTOR independently of myostatin. *J. Cell Biol.* **197**, 997–1008 (2012).
5. Q. Wang, Z. Khayat, K. Kishi, Y. Ebina, A. Klip, GLUT4 translocation by insulin in intact muscle cells: detection by a fast and quantitative assay. *FEBS Lett.* **427**, 193–197 (1998).
6. N. Condon, J. Stow, A. Wall, Automated Analysis of Cell Surface Ruffling: Ruffle Quantification Macro. *BIO-PROTOCOL* **10** (2020).
7. S. H. Raun, *et al.*, Rac1 muscle knockout exacerbates the detrimental effect of high-fat diet on insulin-stimulated muscle glucose uptake independently of Akt. *J. Physiol.* **596**, 2283–2299 (2018).
8. G. Strömblad, P. Björntorp, Reduced hepatic insulin clearance in rats with dietary-induced obesity. *Metabolism* **35**, 323–327 (1986).
9. P. Brandimarti, *et al.*, Cafeteria diet inhibits insulin clearance by reduced insulindegrading enzyme expression and mRNA splicing. *J. Endocrinol.* **219**, 173–182 (2013).
10. S.-H. Jung, C.-H. Jung, G. M. Reaven, S. H. Kim, Adapting to insulin resistance in obesity: role of insulin secretion and clearance. *Diabetologia* **61**, 681–687 (2018).
11. P. Ferre, A. Leturque, A.-F. Burnol, L. Penicaud, J. Girard, A method to quantify glucose utilization in vivo in skeletal muscle and white adipose tissue of the anaesthetized rat. *Biochem. J.* **228**, 103–110 (1985).
12. P. T. Fueger, D. P. Bracy, C. M. Malabanan, R. R. Pencek, D. H. Wasserman, Distributed control of glucose uptake by working muscles of conscious mice: roles of transport and phosphorylation. *Am. J. Physiol. Metab.* **286**, E77–E84 (2004).
13. A. J. Rose, J. Jeppesen, B. Kiens, E. A. Richter, Effects of contraction on localization of GLUT4 and v-SNARE isoforms in rat skeletal muscle. *Am J Physiol Regul Integr Comp Physiol* **297**, 1228–1237 (2009).
14. K. Højlund, *et al.*, Dysregulation of Glycogen Synthase COOH- and NH2-Terminal Phosphorylation by Insulin in Obesity and Type 2 Diabetes Mellitus. *J. Clin. Endocrinol. Metab.* **94**, 4547–4556 (2009).
15. A. Handberg, K. Levin, K. Højlund, H. Beck-Nielsen, Identification of the oxidized low-density lipoprotein scavenger receptor CD36 in plasma: a novel marker of insulin resistance. *Circulation* **114**, 1169–1176 (2006).
16. C. Wang, F. Yue, S. Kuang, Muscle Histology Characterization Using H&E Staining and Muscle Fiber Type Classification Using Immunofluorescence Staining. *Bio-protocol* **7** (2017).
17. E. R. Weibel, Stereological Methods. *Pract. methods Biol. morphometry*, 1–17 (1980).
18. C. Welinder, L. Ekblad, Coomassie Staining as Loading Control in Western Blot Analysis. *J. Proteome Res.* **10**, 1416–1419 (2011).
19. I. Romero-Calvo, *et al.*, Reversible Ponceau staining as a loading control alternative to actin in Western blots. *Anal. Biochem.* **401**, 318–320 (2010).
20. B. S. Antharavally, B. Carter, P. A. Bell, A. K. Mallia, A high-affinity reversible protein stain for Western blots. *Anal. Biochem.* **329**, 276–280 (2004).
21. S. J. Lord, K. B. Velle, R. D. Mullins, L. K. Fritz-Laylin, SuperPlots: Communicating reproducibility and variability in cell biology. *J. Cell Biol.* **219** (2020).
22. L. J. Goodyear, M. F. Hirshman, R. J. Smith, E. S. Horton, Glucose transporter number, activity, and isoform content in plasma membranes of red and white skeletal muscle. *Am. J. Physiol.* **261**, E556-61 (1991).
23. E. J. Henriksen, *et al.*, Glucose transporter protein content and glucose transport capacity in rat skeletal muscles. *Am. J. Physiol. - Endocrinol. Metab.* **259** (1990).

24. M. Kern, *et al.*, Insulin responsiveness in skeletal muscle is determined by glucose transporter (Glut4) protein level. *Biochem. J.* **270**, 397–400 (1990).
25. A. Marette, *et al.*, Abundance, localization, and insulin-induced translocation of glucose transporters in red and white muscle. *Am. J. Physiol.* **263**, C443-52 (1992).
26. L. A. Megeney, *et al.*, Effects of muscle activity and fiber composition on glucose transport and GLUT-4. *Am. J. Physiol.* **264**, E583-93 (1993).
27. K. Bouzakri, *et al.*, siRNA-based gene silencing reveals specialized roles of IRS-1/Akt2 and IRS-2/Akt1 in glucose and lipid metabolism in human skeletal muscle. *Cell Metab.* **4**, 89–96 (2006).
28. M. Friedrichsen, *et al.*, Akt2 influences glycogen synthase activity in human skeletal muscle through regulation of NH2-terminal (sites 2 + 2a) phosphorylation. *Am. J. Physiol. - Endocrinol. Metab.* **304** (2013).
29. B. F. Vind, *et al.*, Hyperglycaemia normalises insulin action on glucose metabolism but not the impaired activation of AKT and glycogen synthase in the skeletal muscle of patients with type 2 diabetes. *Diabetologia* **55**, 1435–45 (2012).